Synthetic modelling study of the effects of CO_2 induced attenuation

Ekanem, A. M., University of Edinburgh and British Geological Survey; Li, X-Y., University of Edinburgh and British Geological Survey; Chapman M., University of Edinburgh and British Geological Survey and Main, I.G, University of Edinburgh*

Summary

We present the results of a synthetic modelling study of the effect of CO_2 induced attenuation. Our theoretical model is made up of four horizontal layers. We computed synthetic seismograms from the isotropic model with no CO_2 saturation and with the third layer of the model comprising of a porous material saturated with water and CO_2 at different concentrations. We used the spectral ratio method to compute the seismic quality factor, Q, from the synthetic data for crack densities of 0.01, 0.02 and 0.03 and zero fracture density at CO_2 saturations of 0 to 100%. The results of our measurement indicate that attenuation is sensitive to CO_2 saturation and crack density. For a given crack density, attenuation increases gradually with decreasing percentage of CO_2 saturation and reaches a maximum at 10% saturation. There is a rapid decrease between CO_2 saturations of 10-30%. Also, the induced attenuation is observed to increase with crack density and offset. No noticeable attenuation is observed for the pure isotropic model with no cracks and fluid saturation.

Introduction

CO_2 is a natural constituent of hydrocarbon reservoirs with saturations varying from 2-80% (Roberts, 2009). At surface temperatures and pressures, CO_2 is in the gaseous phase but exhibits supercritical behavior above the critical point (temperature Tc = 31.1^{o}C and pressure Pc = 7.38 MPa) (David et al, 2008). Attenuation occurs in a fluid saturated rock as a result of squirt flow mechanism (e.g. Mavko and Nur, 1979) and the presence of gas bubble enhances fluid movement, resulting in more attenuation. The presence of CO_2 in the reservoir can result in changes in seismic properties such as travel time, velocity, amplitude and attenuation and thus, an understanding of its influence could be of great importance in the study of hydrocarbon reservoir properties.

In this paper, we have carried out a synthetic modelling study of the effects of CO_2 induced attenuation. Our theoretical model comprises four horizontal layers. We first considered a pure isotropic model with no fluid saturation and then an anisotropic case in the third layer with CO_2 saturations varying from 0-100%. We use the CO_2 properties at the Sleipner field in the North Sea. The field is a site for large scale CO_2 injection project specifically designed as a greenhouse gas mitigation measure (Chadwick et al, 2005). CO_2 have been injected since 1996 into the Utsira Sand reservoir in the field. The Utsira Sand which is saline aquifer has a thickness of 200-300m and CO_2 exists in the reservoir in the supercritical phase (Chadwick et al, 2005). With this model, we aimed to investigate the changes caused by the injection of the CO_2 on P-wave attenuation through the analysis of the seismic response. The results of our attenuation analysis show that attenuation is sensitive to the presence of CO_2, increasing with decreasing percentage of saturation.

Theoretical model and experimental set-up

The theoretical model is made up of four horizontal isotropic layers. To investigate the effects of CO_2, we introduced a porous fluid-saturated material into the third layer and squirt flow between the pores in the matrix is taken into consideration. The material is saturated with water and CO_2 at different degrees of concentrations. 0% CO_2 saturation implies that the material is fully saturated with water while 100% CO_2 saturation means that the material is fully saturated with CO_2. The elastic properties of the porous material are computed using the poroelastic model of Chapman (2003) which considers the pore space of the rock to consist of a collection of spherical pores and circular cracks of small aspect ratio. The pressure difference generated when a seismic wave propagates through the medium causes fluid exchange between the cracks and the surrounding pore space, resulting in attenuation and dispersion. Chapman's (2003) poroelastic model predicts anisotropic velocity dispersion and attenuation in the seismic frequency range, with attenuation increasing with polar angle and azimuth away from the fracture strike. The CO_2 properties are based on the data from the Sleipner field in the North Sea (Chadwick et al, 2005). Details of the model parameters are given in Table 1.

Synthetic data were computed from the theoretical model using the 'ANISEIS' software (Taylor 2001) which makes use of the reflectivity method, for the pure isotropic model case with no cracks and fluid saturation and then for the anisotropic case in the third layer with crack densities of 0.01, 0.02 and 0.03 respectively at various degrees of water and CO_2 saturations ranging from 0-100% and fracture density of 0. A Ricker wavelet with a centre frequency of 25Hz and a start time of 100ms was used as the source wavelet. The source is an explosive source and was placed on the surface of the model. 21 geophones were also placed on the surface of the model, at a regular spacing of 100m, and a source - receiver spacing of 100m was maintained. Data were recorded with a sampling interval of 1ms and a total time of 3s. Sample synthetic gathers are shown in Figure 1 with the reflections from the top and bottom of the fluid-saturated layer highlighted by the red and green arrows respectively.

Table1: Theoretical model parameters

Layer parameters

Layer	**v_p (m/s)**	**v_s (m/s)**	**ρ (Kg/m^3)**	**Thickness (m)**
1	1800	750	1100	400
2	2270	850	2100	600
3	2850	1350	2450	300
4	3800	1800	2600	Half-space

Saturated layer parameters (layer 3)

fracture density	0
CO2 bulk modulus	0.008Gpa
Water bulk modulus	2.305Gpa
porosity	0.37
frequency	50Hz
Relaxation time	5e-3s

Q estimation

We used the spectral ratio method (e.g. Tonn, 1991) to estimate the seismic quality factor, Q from the synthetic data. In each gather, the first trace from the top model reflection at a 0m offset was used as the reference trace for comparison of the spectral ratios. For each trace in the gather and for the top and bottom fluid-saturated layer reflection, we formed the spectral ratios according to Equation 1 and performed a simple least square regression of the Log of the Power Spectral Ratios (LPSR) against frequency.

$$\ln\left(\frac{P_2(f)}{P_1(f)}\right) = 2\ln(\mathrm{RG}) - 2\pi f\left(t_o - t_{ref}\right)/Q \qquad (1)$$

where $P_2(f)$ is the spectral power of the target reflection (top or bottom saturated layer) and $P_1(f)$ is the spectral power of the reference trace, f is the frequency, R is the reflectivity term, G is the geometrical spreading term, t_o is the travel-time of the target reflection, t_{ref} is travel-time of the reference event and Q is the quality factor down to the reflector.

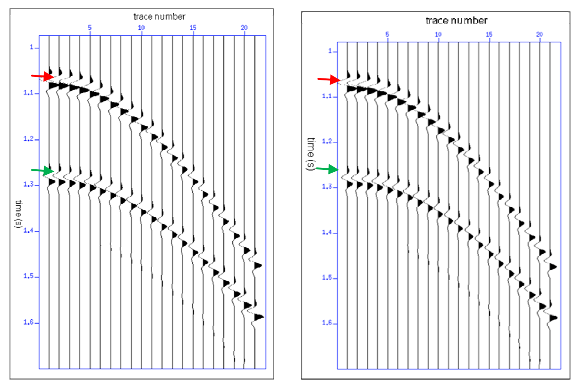

(a) (b)

Figure 1: Sample synthetic gathers: (a) crack density 0.01, CO_2 saturation 0% (b) crack density 0.01 and CO_2 saturation 10%. The red and green arrows indicate the top and bottom reflections respectively from the saturated layer.

We used a constant FFT time window of 180ms to compute the power spectra, and a frequency bandwidth of 20-90Hz where the spectral ratio plots were approximately linear (Figure 2) for the linear regression. The Q down to the reflector was computed from the slope, p of the regression and is given by:

$$Q = 2\pi\left(t_{ref} - t_o\right)/\,p \qquad (2)$$

With the two pair of Q values computed down to the top and bottom of the third layer, we used the layer-stripping method of Dasgupta and Clark (1998) to compute the interval Q value in the third layer using the Equation:

$$Q_i = \frac{[t_n - t_{n-1}]}{t_n/Q_n - t_{n-1}/Q_{n-1}} \qquad (3)$$

where Q_n and Q_{n-1} are the quality factors for the reflectors at the two-way travel times of t_n and t_{n-1} corresponding to the top and bottom of the third layer respectively.

The entire procedure was repeated for all the traces in the gather following the hyperbolic travel path and the average interval Q in the third layer was computed from the mean of all the computed interval Q values in the layer.

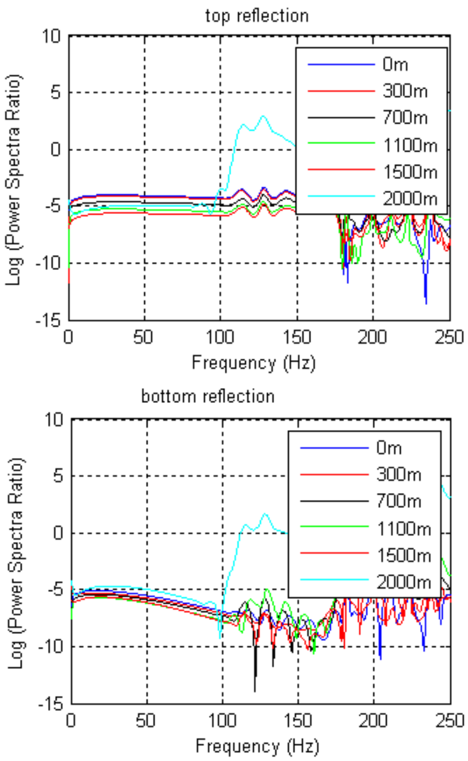

Figure 2: Sample Log Power Spectra Ratio (LPSR) versus frequency plot for crack density 0.01 and 10% CO_2 saturation. The inserted legend indicates the offsets.

Results

The results of our analysis show that higher Q values are obtained in the fluid saturated layer at 0% CO_2 saturation and lower values at 100% CO_2 saturation for the three crack densities considered (Figure 3). The Q values are observed to decrease gradually with decreasing percentage of $C0_2$ saturation from 100-10% for a given crack density, implying more attenuation with decreasing percentage of saturation. The Q values are also observed to decrease systematically with increasing crack density and offset (Figure 3). This implies that the induced P-wave attenuation increases with crack density and offset. There is a remarkable change in the induced attenuation for CO_2 saturations of 10-30%. Beyond this percentage range of saturation, the induced attenuation decreases gradually with increasing percentage of CO_2 saturation (Figure 4). Maximum attenuation occurs at 10% CO_2 saturation. For the pure isotropic case, there is no noticeable attenuation.

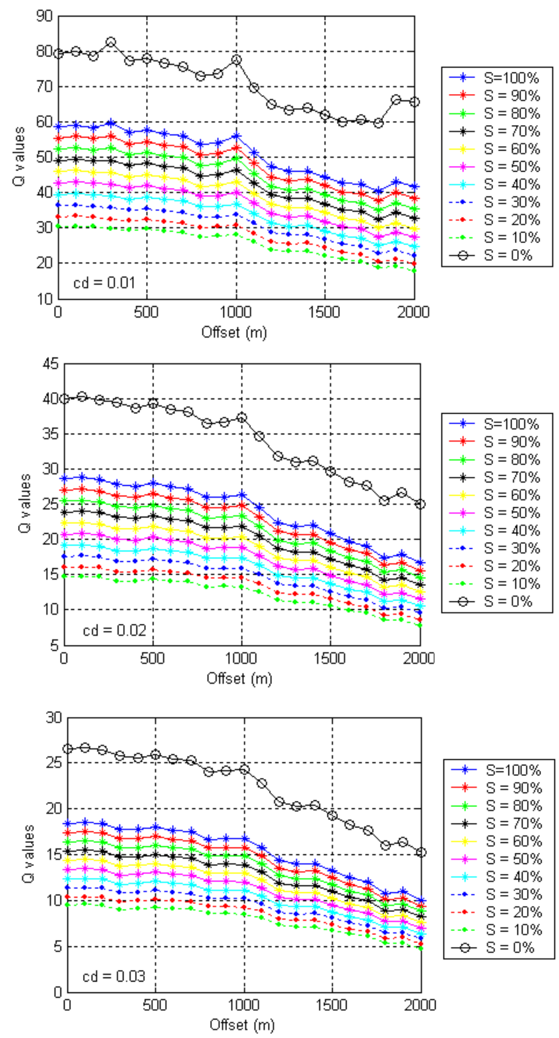

Figure 3: Q profile against CO_2 saturation for different percentages of saturations and crack densities of 0.01, 0.02 and 0.03. The Q values decrease systemically with the percentage of CO_2 saturation and minimum at 10% saturation.

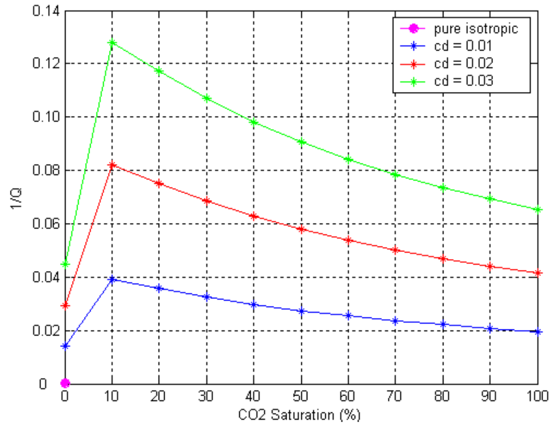

Figure 4: 1/Q profile against CO_2 saturation for different crack densities. No attenuation is observed for the pure isotropic case with no cracks and fluid saturation.

Conclusions

The results of our synthetic modelling study show the sensitivity of P-wave attenuation to CO_2 saturation. P-wave attenuation decreases sharply between CO_2 saturations of 10-30% and gradually beyond this range. The induced attenuation for 100% CO_2 is higher than for 100% water saturation which implies that CO_2 causes more attenuation than water. No account was taken of viscosity effects, thus the model probably overestimates 1/Q for higher percentages of CO_2 saturations. No attenuation is observed in the pure model case where there is no fluid saturation. In the reservoir, the CO_2 is in the supercritical state behaving both as a gas and as a liquid. Partial saturation of CO_2 then causes bubbles which results in more attenuation. The induced attenuation increases with offsets and crack density which is consistent with Chapman's (2003) model.

Acknowledgement

We are grateful to the sponsors of the Edinburgh Anisotropy Project (EAP) for supporting the project and the permission to show the results. Special thanks to the Akwa Ibom State University of Technology (AKUTECH) - Nigeria for providing sponsorship to Ekanem's studies at the University of Edinburgh.

References

Chadwick, R. A., Arts, S. And Eiken O., 2005, 4D seismic quantification of a growing CO_2 plume at Sleipner, North Sea. Petroleum Geology: North-West Europe and Global Perspectives-Proceedings of the 6th Petroleum Geology Conference, 1385–1399.

Chapman M. 2003. Frequency-dependent anisotropy due to meso-scale fractures in the presence of equant porosity. Geophysical Prospecting, **51**, 369-379

Dasgupta, R. and Clark, R., 1998. Estimation of Q from surface seismic reflection data.
Geophysics, **63**(6):2120–2128

David, L.; A. Don; Wright, R,; Dave, M. and Cole, S., 2008. Seismic monitoring of CO2 geo-sequestration: realistic capabilities and limitations. 78th Annual Internal meeting, SEG, Extracted Abstract, 2841-2845.

Mavko, G. M., and Nur, A. (1979). Wave attenuation in partially saturated rocks, *Geophysics,* **44**, 161–178.

Roberts, J., 2009. Developing the Rock Physics Model - Improved Carbon Dioxide Mixing Rules for Carbon Capture and Storage. 71st Conference & Technical Exhibition, EAGE, Expanded Abstract.

Taylor, D., 2001. ANISEIS v5.2 Manual. Applied Geophysical Software Inc., Houston.

Tonn, R., 1991. The determination of the seismic quality Q from VSP data: A comparison of different computational methods. Geophysical Prospecting, **39**, 1- 27